

# Wigner crystallization in a single and bilayer graphene

Hari P. Dahal,<sup>1,2</sup> Tim O. Wehling,<sup>2,3</sup> Kevin S. Bedell,<sup>1</sup> Jian-Xin Zhu,<sup>2</sup> and A. V. Balatsky<sup>2,4</sup>

<sup>1</sup>*Department of Physics, Boston College, Chestnut Hill, MA, 02467*

<sup>2</sup>*Theoretical Division, Los Alamos National Laboratory, Los Alamos, New Mexico 87545*

<sup>3</sup>*I. Institut für Theoretische Physik, Universität Hamburg, Jungiusstraße 9, D-20355 Hamburg, Germany*

<sup>4</sup>*Center for Integrated Nanotechnology, Los Alamos National Laboratory, Los Alamos, New Mexico 87545\**

We study the possibility of Wigner crystallization in both single- and bi-layer graphene using a real space tight binding model. In addition to verifying our earlier prediction for single layer graphene, we predict that the bilayer graphene can undergo a Wigner crystal transition at low enough carrier density thus offering a possibility of tunable and bipolar Wigner crystal. We find that aside from the Coulomb interaction of the carriers of two layers that stabilizes the charge ordered state, so does the inter layer coupling.

PACS numbers:

The study of low dimensional system covers a great deal of area in the research field of physics. In the past couple of years, the experimental success of fabricating single [1, 2] and bi-layer graphene [3] has enriched the interest of studying the properties of low dimensional strongly interacting electronic systems both theoretically and experimentally. The low dimensional system of graphene is more interesting because many of the properties of these systems are quite different from that of the conventional two dimensional system; such as low temperature [3, 4] and room temperature [5] quantum Hall effect, and suppression of weak localization of the carriers [6, 7]. From technological point of view, these systems open up possibilities of atomic-scale electronic devices which can go beyond the limitations of the silicon-based electronics. In addition to the small size of these materials, the very high mobility of the carriers of the single and bilayer graphene looks to be promising for devices which depend up on the transport properties of the carriers.

The importance of studying the single- and bi-layer graphene not only comes from the fact that they have different physical properties compared to the other conventional system such as two dimensional electron gas (2DEG) prepared in the heterostructure of GaAs and InGaAs but also from the fact that their properties are very different between themselves. One of the best example is the experimental verification of the different quantum Hall effect in the single [4] and bilayer graphene [3]. Both single and bilayer system show weak localization effect but with different minimum zero-bias conductivity. The theoretical prediction of the Klein paradox in the single layer graphene is another example [8].

Structurally, graphene has a hexagonal lattice structure having two inequivalent lattice sites, A and B, per unit cell. Bilayer graphene is obtained from two identical single layer graphene with a  $z$ -axis stacking in a specific way known as Bernal stacking [9]. The intra layer nearest-neighbor hopping energy is about ten times stronger than the inter layer hopping. So, to the lowest

order approximation, each layer of the bilayer graphene is almost similar to the single layer graphene, except that the two layers are coupled via small inter layer hopping. The effective difference can be seen in the low energy dispersion relation of the charge carriers in the conduction band which for the single and bilayer graphene can be written as,  $\varepsilon_k = \pm \hbar v_f k$ , and  $E_k = \pm t_{\perp} \pm \sqrt{t_{\perp}^2 + \varepsilon_k^2}$ , [9] respectively, where, we set  $\hbar = 1$ . These dispersion relations are obtained using tight binding model where  $v_F = \frac{3ta}{2} = 5.8eV\text{\AA}$  is the Fermi velocity,  $t = 3.2eV$  is the intra layer nearest-neighbor hopping energy, and  $t_{\perp} = 0.1t$  is the inter layer hopping energy. For bilayer graphene for small  $k$ , the dispersion relation for two of the branches can be approximated as,  $E_k = \pm \frac{k^2}{2m}$ . So due to the inter layer hopping the massless particles of the single layer graphene become massive where the mass of the carriers,  $m$ , is related to inter-layer hopping energy by,  $m = t_{\perp}/v_F^2$ . An important point to note here is that the dispersion relation of the single layer graphene is quite different than that of the 2DEG system whereas the dispersion relation of the bilayer graphene has similar form, i.e., parabolic dispersion, as that of 2DEG system. Flat dispersion in bilayer effectively lowers the kinetic energy for particles with small momenta. This effect will become important for our discussion of Wigner Crystallization (WC).

Here we want to study the charge ordering effects in single versus bilayer graphene. Difference in electronic spectra could manifest itself as a difference in the possible charge ordered states. Indeed we find this to be the case. We find that WC can occur in a bilayer system at small doping limit in zero magnetic field. On the other hand the single layer graphene is stable against charge ordering [10]. WC is a physical phenomenon envisioned by Wigner [11], in which the crystallized phase appears when electrons localize and form a crystal to minimize the potential energy, while paying the concomitant kinetic energy cost which arises from localization. This phase arises in 2DEG system which has parabolic dispersion relation as we decrease the carrier density,  $n$ , of

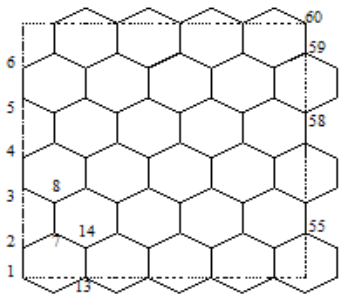


FIG. 1: Lattice structure of graphene single layer having 60 lattice sites that we used to solve the hamiltonian. The index number of some of the lattice sites are shown.

the system because the ratio of the potential to kinetic energy varies as  $\frac{1}{\sqrt{n}}$  which can be made as large as it is needed to get the crystallized phase by making the system more and more dilute.

This discussion brings obvious questions about the WC in graphene: a) Can a single layer graphene have a Wigner crystal phase even if it has linear dispersion relation? b) Is it obvious that the bilayer graphene will have Wigner crystal phase since it has parabolic dispersion relation? c) If bilayer can have crystallized phase what is the structure of the crystallized phase? We will answer these questions by calculating the occupation  $\langle n \rangle$ , of carriers on lattice sites of single and bilayer graphene using a real space tight binding model. If  $\langle n \rangle$  is equal for all sites, we will define the state as homogeneous phase, and if it not equal for all sites, we define the state as some sorts of inhomogeneous phase, one of which is the Wigner crystal phase. We will determine the structure of the inhomogeneous phase with varying  $\langle n \rangle$ .

We now use a real space tight-binding model a) to verify that single layer graphene remains in the liquid phase, and b) to predict that bilayer graphene can undergo a crystallization transition. We study the electronic distribution on the lattice of single layer and bilayer graphene having 60 atomic sites in each layer. The real space distribution of the system of 60 lattice sites that we have chosen and some of the corresponding indices is shown in Fig. 1. In addition to this layer, the bilayer graphene has another layer below or above this layer with a shift of the whole layer by one lattice spacing in the lateral direction. For the second layer we index the lattice sites with indices 61 to 120. We use the real space tight binding hamiltonian.

The tight-binding Hamiltonian to be solved is as follows:

$$H = - \sum_{k=l,i,j} t_{ki,lj} c_{ki}^\dagger c_{lj} - \sum_{k \neq l,i,j} t_{\perp Aki,Alj} c_{Aki}^\dagger c_{Alj} + \frac{1}{2} \sum_{ki \neq lj} V_{ki,lj} n_{ki} n_{lj} + \sum_i V_0 n_{ki\uparrow} n_{ki\downarrow} - \mu \sum_{ki} n_{ki}, \quad (1)$$

where  $i, j$  denote the lattice sites in both single and bilayer, and  $k, l = 1, 2$  represent index for the first or second layer of bilayer graphene. For single layer,  $k = l = 1$ . Since the first term of Hamiltonian has summation over  $i, j$  only for  $k = l$ ,  $t_{ki,lj}$  represents the hopping energy of the electrons only within a layer. We do calculation including only the nearest neighbor hopping with energy equal to  $t_{ki,lj} = t = 3.2eV$  for all lattice sites. For the second term of the Hamiltonian the summation is only for  $k \neq l$  which implies that for single layer graphene this term is zero and for bilayer graphene  $t_{\perp Aki,Alj}$  represents the inter layer hopping energy. In this term  $A$  denotes one of the non-equivalent lattice sites. Since the bilayer graphene can be obtained by the special stacking called the Bernal stacking of two single layers graphene, electrons can hop between two layers only through one of the sublattices which we have chosen to be  $A$ . For the summation of this term, since one of the two layers is shifted laterally by one lattice spacing, if  $i$  is an even numbered lattice index,  $j$  will be an odd numbered lattice index or vice-versa.  $V_0$  is the on site coulomb repulsion,  $V_{ki,lj}$  is the interacting potential between two electrons at position  $r_{ki}$  and  $r_{lj}$ ,  $\mu$  is the chemical potential, and  $n_{ki}, n_{lj}$  are the occupation number of the electrons on lattice sites  $i, j$  of the layer  $k, l$  respectively. Except otherwise indicated, we use  $V_{ki,lj} = \frac{e^2 \exp(-|r_{ki}-r_{lj}|/2a)}{\epsilon(a+|r_{ki}-r_{lj}|)}$ , where  $2a$  is the screening length, so that we could regularize the on-site potential  $V_0 = V_{ki=lj} = \frac{e^2}{\epsilon a}$  to be finite. There are indications that Coulomb terms are decaying faster than  $1/r$  that would also be consistent with our approximation of taking into account only a few lattice sites [12] [13].

We use mean-field theory to simplify the Coulomb interaction term. The Hamiltonian then can be expressed as,

$$H_{MF} = - \sum_{k=l,i,j} t_{ki,lj} c_{ki}^\dagger c_{lj} - \sum_{k \neq l,i,j} t_{\perp Aki,Alj} c_{Aki}^\dagger c_{Alj} + \sum_i (W_{ki} + U_{ki} - \mu) n_{ki} - C, \quad (2)$$

where  $W_{ki} = \sum_{lj} V_{ki,lj} \langle n_{lj} \rangle$ ,  $U_{ki} = \frac{V_0 \langle n_{ki} \rangle}{2}$ ,  $C = \frac{1}{2} \sum_{ki \neq lj} V_{ki,lj} \langle n_{ki} \rangle \langle n_{lj} \rangle + \sum_{ki} V_0 \langle n_{ki\uparrow} \rangle \langle n_{ki\downarrow} \rangle$  is a constant.

Using periodic boundary condition we write down a Hamiltonian matrix corresponding to,

$$h_{ki,lj} = -t_{ki,lj} - t_{\perp Aki,Alj} + (W_{ki} + U_{ki} - \mu) \delta_{ki,lj}, \quad (3)$$

for single and bilayer graphene. For single layer graphene, we calculate  $W_{ki}$  including carriers up to next-next nearest neighbor. For 60 lattice sites in a single layer, the Hamiltonian becomes a  $60 \times 60$  symmetric matrix. For the bilayer graphene also, we calculate the contribution to  $W_{ki}$  coming from both the layers  $k, l$  including the next-next nearest neighbor. The Hamiltonian for the bilayer graphene becomes a  $120 \times 120$  symmetric matrix.

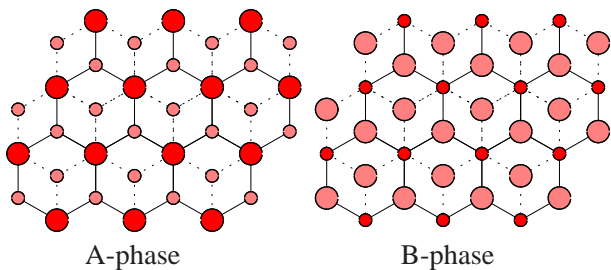


FIG. 2: (Color online) Charge distribution in ordered state of bilayer graphene is shown. Larger circles correspond to larger charge density on lattice sites. The sites connected by solid lines belong to the top layer and by dotted lines belong to bottom layer. The left figure, which we define as A-phase, has charge ordering where larger charge densities are sitting on sub-lattice A. The right figure, which we define as B-phase, has charge ordering where large charge densities are sitting on sub-lattice B.

To find the distribution of electrons on the lattice we start with a random distribution of  $\langle n_{ki} \rangle$ . Using random initial input of  $\langle n_{ki} \rangle$ , we construct  $h_{ki,lj}$  and find the eigenvalues  $E_n$  and eigenvectors  $\phi_{ki}^n$ . We calculate new  $\langle n_{ki} \rangle$  using following relation,

$$\langle n_{ki} \rangle = \sum_n |\phi_{ki}^n|^2 f(E_n), \quad (4)$$

where,  $f(E_n) = 1/(e^{\frac{E_n}{k_B T}} + 1)$  is the Fermi distribution function. Using the standard procedure of the mixing of the old and new  $\langle n_{ki} \rangle$ , we repeat the calculation until we reach the convergence of  $\langle n_{ki} \rangle$ . We check that the results we obtain do not depend on initial distribution of  $n_{ki}$ .

a) *Single layer case.* We calculate occupation number,  $\langle n_i \rangle$ , of electrons on each lattice site of the single layer graphene. We choose different values of the chemical potential and Coulomb potential to vary the average occupation number below half filling and evaluate  $\langle n_i \rangle$  for all  $i$ . We always find  $n_i = n_j$  for all sites. This defines a homogeneous charge distribution also known as the liquid phase. Thus we verify our earlier prediction that the single layer graphene always remains in the liquid phase. Here we remark that this homogeneous phase assumes that graphene sheet has no ripples [14].

b) *Bilayer case.* Similar to the case of single layer graphene, we calculate  $\langle n_i \rangle$  for each lattice site. In bilayer case, in addition to the Coulomb energy and chemical potential, we can tune the inter layer hopping energy,  $t_\perp$ . First we imagine turning off the Coulomb energy and study the charge distribution as a function of  $t_\perp$ . We find that  $\langle n_i \rangle = \langle n_j \rangle$  for all  $j = i + 2$ , and  $\langle n_i \rangle \neq \langle n_j \rangle$  for all  $j = i + 1$ . This implies that all A-sites have equal occupation. Similarly, all B-sites have equal occupation. But, site A and B do not have equal occupation. This defines a commensurate triangular inhomogeneous phase. Since this inhomogeneity is driven only by the inter-layer hopping energy, we define this phase as kinetic energy driven

(KED) inhomogeneous phase. Depending up on the average occupation of the charge carriers on the lattice, also known as filling factor, we find two distinct inhomogeneous phases, KED-A and B phase. A schematic representation of the charge distribution in these two phases is shown in Fig. 2. We find KED-A phase when the filling factor is less than half filling and the KED-B phase when it is more than half filling. We find a cross over between these phases at half filling. So exactly at half filling the system will be in liquid phase.

When we turn off  $t_\perp$  and turn on Coulomb energy, we again find the inhomogeneity in the charge distribution. The charge distribution resembles to that of the B-phase as shown in Fig. 2. Since this phase is driven by the inter-layer Coulomb interaction, we define this phase as a Coulomb interaction driven Wigner crystal (WC) phase. The pattern of the inhomogeneous charge distribution does not change below and above the half filling case; of course the system regains the liquid phase far above the half filling.

If we include both the inter layer Coulomb interaction and the inter layer hopping, we find competing phases below the half filling and cooperating phases above it. Above the half filling KED-B and WC-B phases cooperate with each other. Below the half filling, KED-A and WC-B phases compete with each other. Since this competing phase is more interesting, we are going to explore it more for a system which has 40% filling.

To define the degree of the inhomogeneity of both the A and B phases we define a charge order parameter,  $\Delta = \frac{2(n_B - n_A)}{n_B + n_A}$ . In principle this order parameter is position dependent, but in our calculation it is transactionally invariant. For B-phase it gives a positive number and for the A-phase it gives a negative number. We will be using the absolute value. The result of the calculation of this order parameter as functions of  $t_\perp$  and  $V_0$  is shown in Fig. 3.

For a finite  $V_0$ , an increase in  $t_\perp$  decreases the order parameter of WC-B phase. A further increase in  $t_\perp$  destroys the WC-B phase turning it in to a liquid phase and finally drives the system to a KED-A phase. Similarly, for a finite  $t_\perp$  for zero  $V_0$  the system is in the KED-A phase. Increase in  $V_0$  destroys the KED-A phase turning it to a liquid phase and finally drives the system in to WC-B phase. The black colored region on the figure separates the two competing phases. For realistic parameters we expect  $V_0 \gg t_\perp$  and WC-B state always wins. In practice disorder and fluctuations will produce mixture of these two states in real systems.

How one can detect WC in a bilayer? One experiment that would be sensitive to the charge ordering at atomic scale is scanning tunneling spectroscopy. It would allow one to measure spatial variations of local density of states. To better characterize WC states we calculate the local density of states (LDOS)  $N_k(\mathbf{r}_i, \omega) = \sum_n |\phi_k^n(\mathbf{r}_i)|^2 \delta(\omega - E_n)$ , in the WC phase for bilayer and

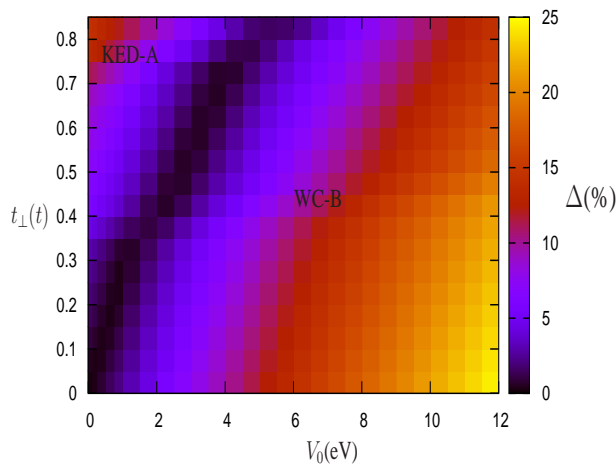


FIG. 3: (Color online) The order parameter of competing KED-A and WC-B phases as functions of  $t_{\perp}$  and  $V_0$  at  $\langle n \rangle = 0.4$ . Increasing  $V_0$  increases the order parameter of WC-B phase, whereas increasing  $t_{\perp}$  increases the order parameter of KED-A phase. The black-colored region represents the phase boundary between these two competing phases.

in liquid phase for a single layer graphene, see Fig. 4.

DC transport measurements is a less direct alternative way to detect WC phase. Depinning effects and other transport anomalies could be another way to detect suggested WC phase.

In conclusion, we show that the single layer graphene always remains in a liquid phase. We also show that the bilayer graphene is bound to undergo Wigner crystallization at reasonable value of the Coulomb interaction. We find that in principle there are two crystallized configurations possible in a bilayer. The in-phase KED-A state is stabilized by interlayer hopping. The out-of-phase WC-B state is stabilized by the Coulomb interactions. LDOS maps, that can be measured with STM, would reveal charge alternations between sites and would allow direct imaging of the WC state in bilayer graphene.

We are grateful to E. Andrei, A. Geim, A. Lichtenstein, M. Katsnelson, A. Morpurgo, A.C. Neto, G. Lee, P. Littlewood and H. Fukuyama for useful discussions. We would like to thank Andrew Heim for his help to develop the code for the iteration. This work has been supported by US DOE.

\* avb@lanl.gov, <http://theory.lanl.gov>

- [1] K. S. Novoselov, A. K. Geim, S. V. Morozov, D. Jiang, Y. Zhang, S. V. Dubonos, I. V. Grigorieva, and A. A. Firsov, *Science* **306**, 666 (2004).
- [2] K. S. Novoselov, D. Jiang, T. Booth, V. V. Khotkevich, S. M. Morozov, and A. K. Geim, *PNSA* **102**, 10451 (2005).
- [3] K. S. Novoselov, E. McCann, S. Morozov, V. Falco, M. I. Katsnelson, U. Zeitler, D. Jiang, F. Schedin, and A. K.

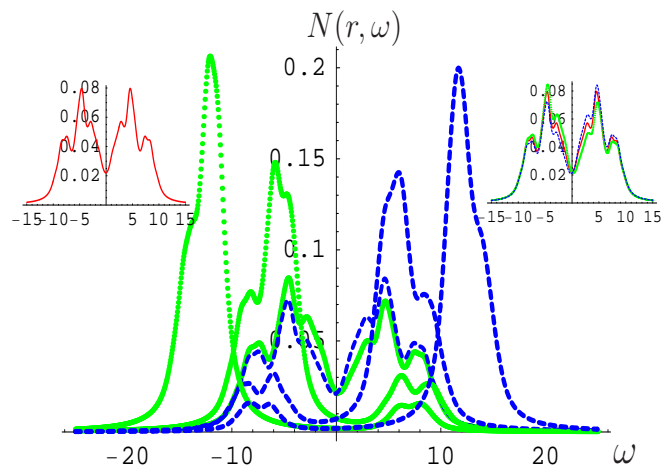


FIG. 4: LDOS of WC phase as a function of energy for various  $\Delta = 0.19, 1.25, 1.75$  and fixed  $t_{\perp} = 0.1t$ . LDOS of sub-lattice A and B in WC-phase is shown in blue (dashed) and green (dotted) curves, respectively. LDOS of a liquid state in a single layer graphene is shown in Red color (solid curve). One can clearly see the linear dependence of DOS on energy that is characteristic of graphene and should be observed for all LDOS in a liquid. The offset on the Y-axis is due to the effect of the Lorentian broadening (half-width =  $0.25t$ ) used to make LDOS curve smooth. LDOS for a WC with  $\Delta = 0.19$  is shown in the upper right figure. If we zoom-in the figure we can see the emergence of the energy gap in the spectrum (that is not fully developed due to finite size effects in our calculations). One also can observe the staggering of the LDOS as a function of energy for nearest neighbor sites. The site with larger charge density will have a larger integrated weight on the negative bias side and vice versa. For  $\Delta = 1.75$  we find fully developed gap in the spectrum (main panel, highest peak) with the same staggering between sublattices in WC. The higher values of  $\Delta$  is obtained by taking larger screening length of the Coulomb potential.

Geim, *Nature Physics* **2**, 177 (2006).

- [4] K. S. Novoselov, A. k. Geim, S. Morozov, D. Jiang, M. I. Katsnelson, I. V. Grigorieva, S. V. Dubonos, and A. A. Firsov, *Nature* **438**, 197 (2005).
- [5] K. S. Novoselov, Z. Jiang, Y. Zhang, S. V. Morozov, H. L. Stormer, U. Zeitler, J. C. Maan, G. S. Boebinger, P. Kim, and A. K. Geim, *Science* **315**, 1379 (2007).
- [6] S. V. Morozov, K. S. Novoselov, M. I. Katsnelson, F. Schedin, L. A. Ponomarenko, D. Jiang, and A. K. Geim, *cond-matt/0603826* (2006).
- [7] R. V. Gorbachev, F. V. Tikhonenko, A. S. Mayorov, D. W. Horsell, and A. K. Savchenko, *cond-matt/0701686* (2007).
- [8] M. I. Katsnelson, K. S. Novoselov, and A. K. Geim, *Nature Physics* **2**, 620 (2006).
- [9] J. Nilsson, A. H. C. Neto, F. Guinea, and N. M. R. Peres, *cond-matt/0604106* (2007).
- [10] H. P. Dahal, Y. N. Joglekar, K. S. Bedell, and A. V. Baltaskey, *Phys. Rev. B* **74**, 233405 (2006).
- [11] E. Wigner, *Phys. Rev.* **46**, 1002 (1934).
- [12] M. I. Katsnelson, *Phys. Rev. B* **74**, 201401 (2006).
- [13] For simplicity of calculation we introduce an exponential cut-off so that potential rapidly drops out at large dis-

tances. This approximation allows us to keep Coulomb interaction between few sites but avoids the difficulty of keeping track for interactions at large distances. Since we find a stable Wigner Crystal phase with the potential we consider we expect longer range Coulomb terms will only

stabilize it more.

- [14] J. C. Meyer, A. K. Geim, M. Katsnelson, K. Novoselov, T. Booth, and S. Roth, *Nature* **446**, 60 (2007).